ChemComm

COMMUNICATION

Functionalised endohedral fullerenes in single-walled carbon nanotubes†

Maria del Carmen Gimenez-Lopez,[a] Andrey Chuvilin,‡[*bc] Ute Kaiser[*d] and
Andrei N. Khlobystov[*a]

Atomically thin carbon nanotubes serve as transparent-test tubes for individual molecules of functionalised endohedral fullerenes. Aberration-corrected transmission electron microscopy reveals the complex dynamic behaviour of these molecules at the atomic level, and it sheds light on the mechanism of their encapsulation into nanotubes.

Fullerenes and single-walled carbon nanotubes (SWNT)—hollow atomically thin nanostructures—are ideal containers for individual atoms and molecules. Highly reactive atomic nitrogen, for example, being encapsulated within a carbon shell of so-called "endohedral" fullerene $N@C_{60}$ can be manipulated and studied in solution under ambient conditions.[1] Similarly, chains of molecules lined up in SWNT can be readily deposited onto various surfaces and integrated in electronic nano-devices.[2] As the technology for entrapment of guest-species within the carbon nano-containers enters chemical sciences, imaging of individual molecules for understanding their structures, verifying their positions and analysis of their dynamic behaviour becomes increasingly important.

Despite recent advances in scanning probe microscopy (AFM and STM),[3–5] the only method that can retrieve atomically resolved volume information (*i.e. seeing through* specimen) is aberration-corrected high-resolution transmission electron microscopy (AC-HRTEM). The energy of the electron beam ("e-beam"), however, must be carefully chosen to avoid radiation damage to the specimen. For example, at e-beam energies below 90 keV, single-walled carbon nanotubes (SWNTs) are stable indefinitely, but more complex structures may be damaged, because the energy threshold for radiation damage depends crucially on the chemical composition and nature of bonding.[6] To minimise the detrimental effects of the e-beam on individual molecules, we utilise SWNTs as atomically thin molecular containers that
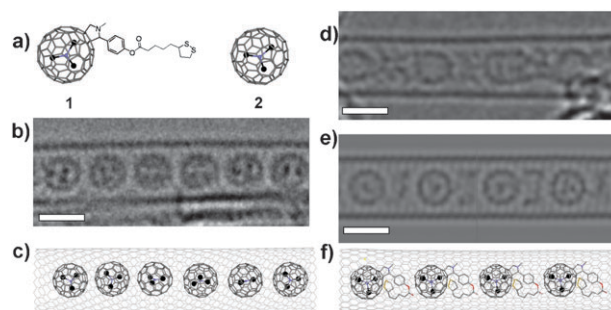
[a] *School of Chemistry, University of Nottingham, Nottingham, NG7 2RD, UK. E-mail: andrei.khlobystov@nottingham.ac.uk*
[b] *CIC nanoGUNE Consolider, Tolosa Hiribidea 76, E-20018 Donostia/San Sebastian, Spain. E-mail: a.chuvilin@nanogune.eu*
[c] *IKERBASQUE, Basque Foundation for Science, 48011, Bilbao, Spain*
[d] *University of Ulm, Central Facility of Electron Microscopy, Albert Einstein Allee 11, 89069, Ulm, Germany. E-mail: ute.kaiser@uni-ulm.de*
† Electronic supplementary information (ESI) available. See DOI: 10.1039/c0cc02929g
‡ All TEM measurements were carried out during AC stay in Ulm.

Fig. 1 (a) Structural diagrams of $M_3N@C_{80}$ **2** and $M_3N@C_{80}$ functionalised with an organic group **1** consisting of a pyrrolidine ring (attached to fullerene), phenyl ester, alkyl and dithiolane group (three metal-atoms arranged in a triangular fashion around the N-atom inside the cage are shown as black circles). (b) Experimental AC-HRTEM image and (c) structural diagram of **2**@SWNT. (d) Experimental AC-HRTEM image (elongated shapes of fullerenes are due to molecular motion on the timescale faster than the image capture rate of *ca.* 1 s), (e) simulated image and (f) structural diagram of **1**@SWNT (scale bars = 1 nm).

simultaneously act as an electromagnetic shield and an effective heat and charge sink (Fig. 1). In our study, we perform AC-HRTEM at 80 kV[7–9] which, combined with the "carbon nano test-tube approach", makes it possible to image molecules with increasingly more complex structures.

80 kV AC-HRTEM imaging within the nanotube works well for a number of simple fullerene molecules (*e.g.* C_{60}, C_{70}, C_{82}, not shown) routinely giving images with atomic resolution. Endohedral fullerenes, such as $M_3N@C_{80}$ (M = Group III element, **2** Fig. 1a and c), which have three degrees of freedom in SWNTs: position along the nanotube axis, orientation of the fullerene cage and orientation of the M_3N cluster with respect to the nanotube axis, can be imaged at 80 keV with comparable resolution but enhanced contrast to that achieved at the higher energy of 120 keV.[10] The endohedral cluster M_3N is particularly prominent in the case of higher Z-value atoms, such as Ho, clearly visible inside the nanotube (Fig. 1b), while for lower Z-value atoms, such as Sc, the endohedral atoms are much harder to observe. However, regardless of the nature of the fullerene, the molecules are densely packed within the SWNT, so that only minimal van der Waals separation of ~ 0.3 nm is observed between the neighbouring species (Fig. 1b and c). As a result of this close packing, translational motion of the fullerene molecules is suppressed

as they remain stationary in the same section of the SWNT, but the orientations of endohedral clusters can still vary as clearly demonstrated in Fig. 1b.

The exterior of endohedral fullerenes can be involved in organic reactions allowing the attachment of functional groups to their carbon cages while retaining the endohedral atoms inside.[11–14] We have utilised the reactivity of $M_3N@C_{80}$ in 1,3-dipolar cycloaddition reactions leading to the attachment of a pyrrolidine group, which we designed to bear a complex organic group consisting of a phenyl ester moiety linked through a C4 alkyl chain to a dithiolane group 1 (Fig. 1a). Such functionalisation of $Sc_3N@C_{80}$ 1 adds conformational flexibility of the organic group as another degree of freedom within SWNT.

Using 80 kV AC-HRTEM we are able to visualise individual molecules 1 inside the nanotube (Fig. 1d). The molecules appear to form a chain with periodic spacing between the fullerene cages, which is twice greater than that for unfunctionalised fullerene $M_3N@C_{80}$. The increase of the inter-fullerene separation beyond the typical van der Waals contact of 0.34 nm is dictated by the size of the functional group, which adopts a folded conformation within the nanotube (Fig. 1f). This inter-fullerene separation appears to be very consistent (e.g. Fig. 3e) indicating that the majority of molecules 1 maintain the same cage-to-tail orientation. This observation gives a unique insight into the mechanism of encapsulation of functionalised fullerenes. While the molecule is in solution, it is expected that the fullerene cage of 1 will have a significantly higher attraction to the nanotube than its functional group[15] which will steer this molecule to enter the nanotube "cage first" (Fig. 2). Our previous studies of the functionalised fullerene C_{60} in nanotubes[16,17] typically showed no preferential orientation. The different behaviour of 1 may be explained by the fact that the C_{80} fullerene cage can form stronger interactions with the nanotube interior than C_{60} because of a larger size and a more polarisable nature of C_{80} as compared to C_{60}. As a result, C_{80} would form stronger and more long-range van der Waals interactions with the nanotube as compared to the C_{60} analogues, leading to an orientational selectivity for encapsulation of molecule 1. As the molecules are not able to turn around inside the nanotube channel because of their high aspect ratio, this encapsulation mechanism will result in a periodic "cage-to-tail" structure observed in Fig. 2b.
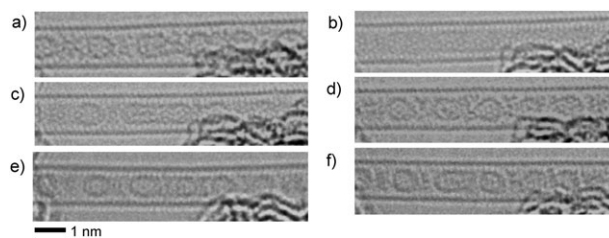
Fig. 3 A time series of 80 kV AC-HRTEM images showing molecule 1 becoming blurred (b, c) from time to time due to its translational motion on the timescale faster than the image capture rate of about 1 s.

Since the functional group of 1 acts as a flexible spacer between fullerene cages, any thermally or e-beam induced vibrations or changes in conformation of the group will cause movement of the molecules along the SWNT axis (translational motion). Any motion on the timescale faster than the image capture rate (ca. 1 s) will lead to delocalisation of the observed atomic positions, yielding in blurred images of the molecule (Fig. 3b and c), which appears to be significantly more pronounced for 1 than for the unfunctionalised endohedral fullerenes 2 that possess fewer degrees of internal freedom (compare Fig. 1b and Fig. 3). Simulated TEM images taking into account the motion of the molecule match well the observed images (Fig. 1e and ESI†).

Even though the energy of e-beam was lowered to 80 keV, radiation damage effects were sufficiently strong to trigger the fragmentation of the functional group of 1. It is interesting that the fragmentation of the organic group in TEM follows the same pathway as esters under the e-beam of a mass spectrometer[18] (Fig. 4a). In both cases the impact of the e-beam ionises the molecule and forms a cation-radical (Fig. 4a), which undergoes a hydride transfer from the α-carbon to the ester oxygen leading to a cleavage of the alkyl ester part of the functional group.

A shorter, more rigid pyrrolidine-phenoxy group remaining attached to the fullerene cage can be clearly seen by AC-HRTEM (Fig. 4b). Surprisingly, the endohedral cluster Sc_3N becomes visible only when the functional group of 1 is fragmented, which may be related to a charge on the oxygen atom of the residual pyrrolidine-phenoxy group (Fig. 4a) that creates a local electric field, slowing down the rotational motion of Sc_3N as compared to the original compound 1.
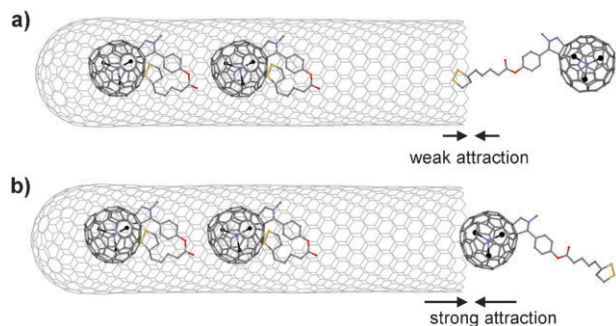

Fig. 2 Van der Waals interactions of the fullerene cage (b) with the opening of carbon nanotube are significantly stronger than with the functional group (a) leading to a preferential encapsulation of the molecule 1 in a "cage-first" fashion.
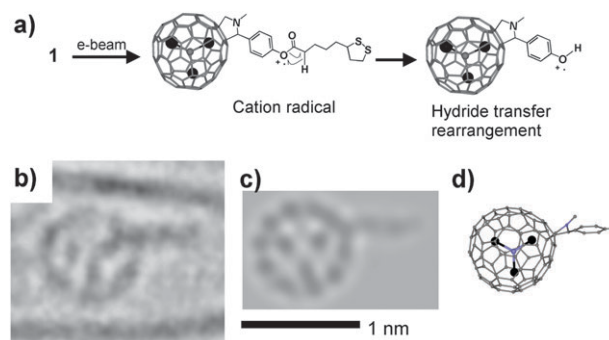

Fig. 4 On the impact of the e-beam, the exohedral functional group of 1 dissociates at the C–O bond of the ester group (a). (b) Experimental and (c) simulated 80 kV TEM images of the fullerene 1 after the fragmentation where the endohedral cluster Sc_3N becomes visible. (d) Orientation of the fragment used for image simulation.

This is the first example of direct visualisation of endohedral atoms with respect to an exohedral functional group. The endohedral Sc_3N cluster exhibits near free rotation in an unmodified $Sc_3N@C_{80}$,[19] but when a functional group is attached to the C_{80} cage, the rotation of Sc_3N is more restricted. It is reported to adopt different orientations with respect to the exohedral group depending on the nature of that group,[20,21] which is difficult to determine by conventional spectroscopic methods.[22,23] X-Ray diffraction analysis appears to be more informative, but it provides only information about the "average" orientation of the M_3N group for a large number of molecules in the crystal that typically exhibit some structural disorder.[13,20] AC-HRTEM offers a glimpse at the atomic structures of individual molecules revealing that one of the scandium atoms of Sc_3N is oriented towards the pyrrolidine group attached to the C_{80}-cage surface (Fig. 4d), which is a new type of orientation unseen previously for this type of molecules.

Carbon nanotubes are ideal low-contrast, atomically thin containers for visualising structurally complex and dynamically active molecules. 80 kV aberration-corrected microscopy simultaneously provides both, structural information about the exterior (functional groups) and the interior of individual fullerenes molecules, at the near-atomic level in direct space and real time. However, radiation damage effects at 80 kV still break organic groups susceptible to ionisation followed by dissociation (*e.g.* ester group). The challenge of the limited stability of the molecules under the e-beam and the fast molecular motion are now tackled in our research *via* four main routes: (1) reduction of the electron energy below 80 keV while increasing the resolution,[7] (2) lowering the dose of electrons onto the specimen in HRTEM mode, (3) cooling the specimen, (4) employing faster and more sensitive electron detectors. If successful, this methodology will revolutionise the way we study molecules.

4-(Liponyloxy)benzaldehyde was synthesized according to the literature.[14] Details of synthesis of *N*-methyl-2-(4-(liponyloxy)-benzyl)-[5,6]-$Sc_3N@C_{80}$ fulleropyrrolidine (**1**) are in the ESI.† The structure of **1** was verified by spectroscopy prior to insertion into nanotubes: MALDI-MS 1447.14 *m/z* [M]$^-$. ^{1}H NMR {500 MHz, $CDCl_3$: CS_2 (1 : 6), 300 K} δ_H 4.38 (d, J = 9.7 Hz, 1H, $-CH_2$ pyrrolidine), 3.76 (s, 1H, $-CH$ pyrrolidine), 3.15 (s, 3H, $-NCH_3$), 3.08 (d, J = 9.7 Hz, 1H, $-CH_2$ pyrrolidine) ppm. Heteronuclear Multiple Quantum Correlation (HMQC) {500 MHz, $CDCl_3$: CS_2 (1 : 6), 300 K} δ_C 85.0 ($-CH_2$ pyrrolidine), 72.5 ($-CH$ pyrrolidine), 41.4 ($-NCH_3$) ppm.

Compound **1** was inserted into nanotubes at room temperature from supersaturated chloroform solution (details are in the ESI†).

TEM investigation was performed on Titan 80–300 (FEI, Netherlands) instrument equipped with an imaging side aberration corrector. The instrument was operated at 80 kV accelerating voltage. In order to decrease the influence of the chromatic aberration, which is the resolution limiting factor at 80 kV, the extractor voltage of the electron gun was decreased to approximately 2000 V, resulting in a better beam monochromaticity. The coefficient of the spherical aberration C_s of the objective lens was set to approximately $+20$ μm and a defocus of -13 nm was used (slightly below Scherzer defocus) in order to increase the contrast. The images were zero-loss filtered using GIF Tridiem (Gatan, USA) and acquired by a Gatan Ultrascan 2 K × 2 K CCD camera. The exposition time was 1 s with intervals of ~2 s between the images. Hardware binning × 2 was used for faster frame rate and to suppress the influence of the modulation transfer function (MTF) of the camera. Significant oversampling (0.023 nm per pix) was used in order to suppress further the influence of the MTF.

Notes and references

1 J. J. L. Morton, A. M. Tyryshkin, A. Ardavan, K. Porfyrakis, S. A. Lyon and G. A. D. Briggs, *J. Chem. Phys.*, 2006, **124**, 014508.
2 D. Obergfell, J. C. Meyer, M. Haluska, A. N. Khlobystov, S. Yang, L. Fan, D. Liu and S. Roth, *Phys. Status Solidi B*, 2006, **243**, 3430.
3 M. Matena, A. Llanes-Pallas, M. Enache, T. Jung, J. Wouters, B. Champagne, M. Stöhr and D. Bonifazi, *Chem. Commun.*, 2009, 3525.
4 T. Kudernac, S. Lei, J. A. A. W. Elemans and S. De Feyter, *Chem. Soc. Rev.*, 2009, **38**, 402.
5 D. Bonifazi, C. Nacci, R. Marega, S. Campidelli, G. Ceballos, S. Modesti, M. Meneghetti and M. Prato, *Nano Lett.*, 2006, **6**, 1408.
6 R. F. Egerton, P. Li and M. Malac, *Micron*, 2004, **35**, 399.
7 H. H. Rose, *Philos. Trans. R. Soc. London, Ser. A*, 2009, **367**, 3809.
8 Z. Liu, K. Suenaga and S. Iijima, *J. Am. Chem. Soc.*, 2007, **129**, 6666.
9 A. Chuvilin, A. N. Khlobystov, D. Obergfell, M. Haluska, S. Yang, S. Roth and U. Kaiser, *Angew. Chem., Int. Ed.*, 2010, **49**, 193.
10 Y. Sato, K. Suenaga, S. Okubo, T. Okazakai and S. Iijima, *Nano Lett.*, 2007, **7**, 3704.
11 E. B. Iezzi, J. C. Duchamp, K. Harich, T. E. Glass, H. M. Lee, M. M. Olmstead, A. L. Balch and H. C. Dorn, *J. Am. Chem. Soc.*, 2002, **124**, 524.
12 M. A. G. Jones, D. A. Britz, J. J. L. Morton, A. N. Khlobystov, K. Porfyrakis, A. Ardavan and G. A. D. Briggs, *Phys. Chem. Chem. Phys.*, 2006, **8**, 2083.
13 L. Echegoyen, C. J. Chancellor, C. M. Cardona, B. Elliott, J. Rivera, M. M. Olmstead and A. L. Balch, *Chem. Commun.*, 2006, 2653.
14 M. C. Gimenez-Lopez, J. A. Gardener, A. Q. Shaw, A. Iwasiewicz-Wabnig, K. Porfyrakis, C. Balmer, G. Dantelle, M. Hadjipanayi, A. Crossley, N. R. Champness, M. R. Castell, G. A. D. Briggs and A. N. Khlobystov, *Phys. Chem. Chem. Phys.*, 2010, **12**, 123.
15 (*a*) H. Ulbricht, G. Moos and T. Hertel, *Phys. Rev. Lett.*, 2003, **90**, 095501; (*b*) M. Yoon, S. Berber and D. Tománek, *Phys. Rev. B*, 2005, **71**, 155406; (*c*) M. Hodak and L. A. Girifalco, *Phys. Rev. B*, 2003, **67**, 075419.
16 T. W. Chamberlain, R. Pfeiffer, H. Peterlik, H. Kuzmany, F. Zerbetto, M. Melle-Franco, L. Staddon, N. R. Champness, G. A. D. Briggs and A. N. Khlobystov, *Small*, 2008, **4**, 2262.
17 T. W. Chamberlain, A. Camenisch, N. R. Champness, G. A. D. Briggs, S. C. Benjamin, A. Ardavan and A. N. Khlobystov, *J. Am. Chem. Soc.*, 2007, **129**, 8609.
18 *NIST Chemistry WebBook, NIST Standard Reference Database Number 69*, ed. P. J. Linstrom and W. G. Mallard, National Institute of Standards and Technology, Gaithersburg MD, 2005.
19 J. M. Campanera, C. Bo, M. M. Olmstead, A. L. Balch and J. M. Poblet, *J. Phys. Chem. A*, 2002, **106**, 12356.
20 H. M. Lee, M. M. Olmstead, E. Iezzi, J. C. Duchamp, H. C. Dorn and A. L. Balch, *J. Am. Chem. Soc.*, 2002, **124**, 3494.
21 A. Rodriguez-Fortea, J. M. Campanera, C. M. Cardona, L. Echegoyen and J. M. Polet, *Angew. Chem., Int. Ed.*, 2006, **45**, 8176.
22 C. M. Cardona, A. Kitaygorodskiy, A. Ortiz, M. A. Herranz and L. Echegoyen, *J. Org. Chem.*, 2005, **70**, 5092.
23 T. Cai, Z. Ge, E. B. Iezzi, T. E. Glass, K. Harich, H. W. Gibson and H. C. Dorn, *Chem. Commun.*, 2005, 3594.